Aquatic Toxicology 241 (2021) 105988

Contents lists available at ScienceDirect

Aquatic Toxicology

journal homepage: www.elsevier.com/locate/aqtox

Exposure to *Deepwater Horizon* crude oil increases free cholesterol in larval red drum (*Sciaenops ocellatus*)

Victoria McGruer [a,b,*], Alexis J. Khursigara [c], Jason T. Magnuson [b], Andrew J. Esbaugh [c], Justin B. Greer [d,b], Daniel Schlenk [b]

[a] *Environmental Toxicology Graduate Program, University of California, Riverside, CA, United States*
[b] *Department of Environmental Sciences, University of California, 2460A Geology, Riverside, CA 92521, United States*
[c] *Marine Science Institute, The University of Texas at Austin, Port Aransas, TX, United States*
[d] *US Geological Survey, Western Fisheries Research Center, Seattle, WA, United States*

ARTICLE INFO

Keywords:
Crude oil
Red drum
Cholesterol
Polycyclic aromatic hydrocarbons
Developmental toxicity
Deepwater Horizon

ABSTRACT

The 2010 *Deepwater Horizon* oil spill impacted over 2100 km of shoreline along the northern Gulf of Mexico, which coincided with the spawning season of many coastal species, including red drum (*Sciaenops ocellatus*). Red drum develop rapidly and are sensitive to crude oil exposure during the embryonic and larval periods. This study investigates the predictions from recent transcriptomic studies that cholesterol biosynthetic processes are impacted by oil exposure in fish early life stages. We found that red drum larvae exposed for 72 h to ΣPAH_{50} 3.55–15.45 μg L^{-1} exhibited significantly increased pericardial area, a cardiotoxicity metric, but the expression of several genes targeted in the cholesterol synthesis pathway was not affected. However, whole-mount staining revealed significant increases in free cholesterol throughout the larval body (ΣPAH_{50} 4.71–16.15 μg L^{-1}), and total cholesterol followed an increasing trend (ΣPAH_{50} 3.55–15.45 μg L^{-1}). Cholesterol plays a critical role in fish embryo development and ion channel function. Therefore, the disruption of cholesterol homeostasis, as observed here, could play a role in the oil toxicity phenotype observed across many fish species.

1. Introduction

The 2010 *Deepwater Horizon* (*DWH*) oil spill released over 3 million barrels of oil offshore into the Gulf of Mexico, making it the largest oil spill in US history to date (Trustees, 2016). While pelagic habitats were immediately impacted, with time, crude oil was pushed to the northern shore of the Gulf of Mexico and oiled at least 2113 km of coastline (Nixon et al., 2016), including nearshore nursery habitats for red drum (*Sciaenops ocellatus*). One year post-spill, moderate to heavy oiling persisted on 78 km of coastline (Michel et al., 2013), suggesting that nearshore species could have been exposed to oiling in some regions for multiple spawning seasons.

Developing embryos are especially vulnerable to crude oil exposure as they are rapidly forming organ systems that will define organism function for the remainder of the individual's life. While post-metamorphosis fish (juveniles and adults) are also susceptible to oil exposure, they have additional defenses such as a fully developed liver and scales that can provide protection that embryos and larvae do not have (Incardona and Scholz, 2018). The *DWH* oil spill coincided with the breeding season of many fish species native to the Gulf (Rooker et al., 2013), including red drum, which spawn nearshore in late summer and early fall. Red drum are ecologically and economically valuable and a managed fishery within the Gulf region (National Marine Fisheries, 2018).

Many fish early life stages, including red drum, display a conserved toxicity phenotype following oil exposure. This phenotype is characterized by cardiotoxicity, including pericardial edema, bradycardia, reduced stroke volume, and reduced cardiac output (Incardona and Scholz, 2018; Khursigara et al., 2017). Embryonic and larval cardiotoxicity due to oil exposure has been linked to reduced swimming performance in surviving juvenile and adult fish (Hicken et al., 2011; Incardona et al., 2015; Mager et al., 2014). Current evidence points to the impairment of ion transport in the heart as a key contributor to oil-induced cardiotoxicity (Brette et al., 2014, 2017). However, the molecular mechanisms underlying the disruption of ion movement and other outcomes such as impaired vision due to oil exposure are currently unknown. Understanding the mechanisms that result in these outcomes can help us predict species sensitivity, develop biomarkers, and generate

* Corresponding author at: Department of Environmental Sciences, University of California, 2460A Geology, Riverside, CA 92521, United States.
E-mail address: victoria.mcgruer@email.ucr.edu (V. McGruer).

https://doi.org/10.1016/j.aquatox.2021.105988
Received 21 May 2021; Received in revised form 27 August 2021; Accepted 29 September 2021
Available online 6 October 2021

risk assessments.

Transcriptomic analyses allow for a broad look at the organismal response to toxicant exposure, reducing bias when hypothesizing about potential toxicity mechanisms. Comparing recent transcriptomic studies, cholesterol-related pathways are consistently enhanced in the early life stages of several marine fish exposed to crude oil (Jones et al., 2020; Sørensen et al., 2017; Xu et al., 2016), including in red drum (*Sciaenops ocellatus*) (Xu et al., 2017). Cholesterol plays a critical role in fish development, and zebrafish (*Danio rerio*) embryos exposed to cholesterol-reducing drugs develop a similar phenotype as those exposed to oil. Pharmaceutical mediated cholesterol reduction induces cardiotoxicity, presenting as pericardial edema and bradycardia, as well as smaller heads and reduced eye area (Maerz et al., 2019). Additionally, bradycardia induced by phenanthrene – a polycyclic aromatic hydrocarbon (PAH) found in crude oil – can be partially rescued by pretreatment with cholesterol, further indicating that cholesterol may contribute to oil-induced toxicity (McGruer et al., 2021). Previous work in mahi-mahi (*Coryphaena hippurus)* embryos exposed to crude oil demonstrated a significant reduction in total cholesterol at 96 h post-fertilization (hpf) (McGruer et al., 2019). Furthermore, oil-exposed yolk-sac-stage polar cod (*Boreogadus saida*) homogenates presented significant increases in sterols (Laurel et al., 2019). However, these studies did not account for the unused yolk-sac or different cholesterol pools available to the developing larvae.

Cholesterol homeostasis is critical for early fish development. The present study investigated whether the predicted transcriptional response translated into a disruption of cholesterol homeostasis in red drum larvae. Using oil collected from the *DWH* surface slick at concentrations that induce visible cardiotoxicity, we first assessed the regulation of the cholesterol synthesis pathway using quantitative polymerase chain reaction (qPCR). Next, we quantified total cholesterol in whole larval homogenates and visualized the free cholesterol distribution and concentration through whole-mount staining. Free cholesterol can be readily incorporated into cell membranes. However, total cholesterol is a measure of both free cholesterol and cholesterol esters, a storage form of cholesterol (Tabas, 2002). Through these methods, we examine how oil affects different pools of cholesterol at a stage when the yolk has been absorbed, but feeding has not yet commenced. Together these results give insight into the role cholesterol may play in developmental toxicity.

2. Material and methods

2.1. Animals

Red drum broodstock were maintained at the Texas Parks and Wildlife-CCA Marine Development Center in Corpus Christi, TX. Following fertilization, red drum embryos were collected and then transferred with aeration to the University of Texas Marine Science Institute. Embryos were handled and visually assessed as described in Khursigara et al. (2017). Briefly, embryos were treated with formalin (1ppt) for 1 h before oil exposure, embryo quality and viability were visually assessed, and spawns with minimal fertilization or viability were not used.

2.2. DWH oil exposure

Red drum embryos were exposed to naturally weathered oil from the surface (OFS) by preparing high-energy water-accommodated fractions (HEWAFs). OFS was collected from the Gulf of Mexico on June 29, 2010, from the hold of barge CT02404 and used to create two sets of exposures. The first set of exposures were initiated on November 12, 2018, hereafter referred to as "exposure 1″. The second exposure began on July 19, 2019, hereafter "exposure 2″. HEWAF solutions for both exposures were produced as previously described in Incardona et al. (2013) using a commercial blender. 1 g of oil was loaded per liter of seawater (35 ppt). Nominal concentrations of 0.625%, 1.25%, and 2.5% HEWAF were produced by diluting the 100% HEWAF with seawater. These concentrations were chosen to mimic previous studies which observed minimal impacts to survival (Khursigara et al., 2017) and predicted changes to cholesterol synthesis (Xu et al., 2017) at similar concentrations. Exposures were conducted in 1 L beakers with 40 embryos for exposure 1 and 30 embryos for exposure 2 per beaker, with treatments starting at 12 hpf. Each concentration contained six test replicates. Exposures were maintained at 25 °C and 35 ppt salinity with a 14 h:10 h light:dark photoperiod. Survival was evaluated daily. All endpoints were assessed at 72 hpf when red drum larvae had nearly depleted their yolk-sac but had not yet transitioned to exogenous feeding. A timeline of exposure duration and red drum early life development is provided in supplemental Fig. 1. All experiments were conducted per the University of Texas at Austin Institutional Animal Care and Use Committee (IACUC) approved protocols (AUP-2014-00375).

2.3. PAH analysis

ΣPAH_{50} concentrations were determined following protocols described by Xu et al. (2017). First, diluted HEWAF solutions were sampled immediately after preparation for PAH analysis. Samples were stored at 4 °C in 250 mL amber bottles until analysis by ALS Environmental (Kelso, WA). Gas chromatography/mass spectrometry-selective ion monitoring (GC/MS-SIM) was used to quantify 76 individual PAHs. A subset of 50 PAH analytes were then totaled to determine the reported ΣPAH_{50} concentrations. Separate HEWAF dilutions were made for exposures 1 and 2, each with three dilutions. Slight differences in the dilutions resulted in the six ΣPAH_{50} concentrations reported in this study. PAH concentrations of the 50 analytes measured are graphically represented in Supplemental Fig. 4. Temperature, pH, dissolved oxygen, and salinity were measured daily and are reported in Supplemental Table 2.

2.4. Morphological assessment

Morphological assessments, gene expression, and total cholesterol quantification were conducted on larvae from exposure 1. At 72 hpf, a subset of larvae (5 individuals per test replicate) were anesthetized in 250 mg L^{-1} MS222 (buffered with 500 mg L^{-1} NaHCO3) for imaging. Larvae were oriented laterally in 3% methylcellulose and imaged using a Nikon SMZ800N microscope and a Nikon Digital Sight DS U-3 instrument. Two-dimensional pericardial area was quantified as a metric of sublethal cardiotoxicity using ImageJ (version 1.53c). Representative images outlining the region measured can be found in Supplemental Fig. 2.

2.5. RNA extraction and quantitative PCR

The remaining exposure 1 larval (72 hpf) test replicates were pooled with another test replicate of the same treatment to create a biological replicate (2 test replicates per biological replicate; $n = 3$ biological replicate per treatment). Biological replicates were equally divided for qPCR analysis and total cholesterol quantification.

Total RNA was extracted for qPCR from larval homogenates using the RNeasy Mini kit from Qiagen (Valencia, CA) and associated protocols. A NanoDrop (Thermo Fisher Scientific; model ND-1000) was used to assess RNA quality and quantity, and RNA was stored at −80 °C. Complementary (c)DNA was reversed transcribed from 1 μg of total RNA using the Promega Reverse Transcription System kit (Madison, WI). cDNA was diluted with nuclease-free water and subsequently stored at −20 °C until qPCR was performed.

The relative mRNA expression of several key genes involved in cholesterol synthesis was assessed in 72 hpf red drum larval homogenates exposed to ΣPAH_{50} 0, 3.55, and 15.45 μg L^{-1}. Primers for 3-hydroxy-3-methylglutaryl-coenzyme A reductase (*hmgcr*), farnesyl-

diphosphate farnesyltransferase 1 (*fdft1*), and squalene epoxidase (*sqle*) were designed using NCBI Primer-BLAST. Primers for *β-actin* were obtained from Hu et al. (2010). Primers for elongation factor 1 α (*ef1-α*) were obtained from Sun and Chi (2016). Primer sequences and amplicon length are provided in Supplemental Table 1. qPCR analysis of all genes was performed using the thermocycling conditions described in McGruer et al. (2019): 95 °C for 5 min, followed by 40 cycles of 95 °C for 10 s and 60 °C for 30 s. Data were normalized to the geometric mean of *ef1-α* and *β-actin* and analysed using the $2^{-\Delta\Delta CT}$ method (Livak and Schmittgen, 2001). Melt curves and 1.2% agarose gel electrophoresis were used to assess product formation and primer specificity.

2.6. Total cholesterol quantification

Total cholesterol, which encompasses cholesteryl esters and free cholesterol, was quantified in whole larval homogenates as described in McGruer et al. (2019). The Cell Biolabs, Inc. (San Diego, CA) "Total Cholesterol Assay Kit (Colorimetric)" and associated "tissue lysates" protocol was used for lipid extraction and total cholesterol quantification. Three biological replicates from exposure 1 were evaluated per treatment with 30–35 larvae per replicate. To summarize, larvae were homogenized in 200 µL chloroform:isopropanol:Triton x-100 (7:11:0.1) to extract lipids. Cholesterol standards provided with the assay kit were used to prepare standard curves and calculate total cholesterol (µg) in each sample. Total cholesterol was normalized to total protein (mg) to account for intersample variability. The total protein of extracted samples was quantified with the Pierce™ BCA Protein Assay Kit (Thermo Scientific, Rockford, IL).

2.7. Filipin staining

Filipin is a naturally fluorescent biomolecule that binds free 3-*β*-hydroxysterols and is a well-established reporter molecule used to detect free cholesterol in cells and tissues (Gimpl and Gehrig-Burger, 2007). Filipin has been previously used to visualize free cholesterol in whole-mount zebrafish larvae (Hölttä-Vuori et al., 2008; McGruer et al., 2021). Filipin staining does not allow for the quantification of free cholesterol concentrations, and the use of three-dimensional samples, rather than thin tissue sections, likely increases the variability of the metric. However, staining whole-mount red drum larvae provides information about the distribution and relative concentration of free cholesterol in the larvae, separate from cholesterol esters.

Here, filipin staining was conducted on larvae from exposure 2. Thirty, 72 hpf larvae were pooled per replicate (Control $n = 3$; Oil exposed $n = 5$ or 6) and fixed in zinc-based formalin Z-fix for 24 h (Anatech LTD). Larvae were then transferred to 1x phosphate buffer solution (PBS) for storage until staining. Fixed larvae were subsequently stained with the cholesterol reporter molecule filipin using previously described protocols (McGruer et al., 2021). Fourteen larvae were included in each staining basket. Larvae were imaged immediately following the completion of the staining protocol to prevent signal loss. Precautions were taken to minimize unnecessary light in the room where imaging was conducted, and each larva was mounted in 4% methylcellulose and imaged individually to minimize photobleaching. Images were collected under both transmitted and UV light.

The larval body was outlined in the image taken under transmitted light and then overlayed on the fluorescent image to quantify mean fluorescence within the larval body using ImageJ (representative outlines provided in Supplemental Fig. 3). Background corrected fluorescence values were calculated by subtracting the mean background fluorescence (3 individual measurements) from the mean larval fluorescence.

2.8. Statistical analysis

Statistical analyses were conducted in R (R Core Team 2020). Assumptions of normality were assessed using Shapiro Wilk's test. Homogeneity of variances was determined using Levene's test. Differences in relative gene expression, filipin staining intensity, and total cholesterol were evaluated by one-way analysis of variance (ANOVA). If the ANOVA revealed statistical differences, multiple comparisons were assessed using Tukey's honest significant difference test. Survival and pericardial area data were analysed by the nonparametric Kruskal-Wallis test followed by Dunn's Test of Multiple Comparisons due to violations of ANOVA assumptions. A significant difference was accepted at $p < 0.05$. All data are presented as means ± standard error of the mean (SEM).

3. Results

3.1. Oil composition

ΣPAH_{50} concentrations determined from OFS HEWAF dilutions were similar across the two sets of exposures. Analysis of the exposure 1 HEWAF diluted to 0.625% HEWAF, 1.25% HEWAF, and 2.5% HEWAF revealed ΣPAH_{50} concentrations of 3.55, 7.45, and 15.45 µg L^{-1}, respectively. The same dilutions produced slightly higher concentrations in the exposure 2 HEWAF, which yielded ΣPAH_{50} concentrations 4.71, 8.15, 16.15 µg L^{-1}, respectively. Across both sets of exposures and all dilutions, three-ring PAHs (i.e., phenanthrenes/anthracenes) dominated the quantified PAH component of the HEWAF, comprising ~ 68–80% of total PAHs (Supplemental Fig. 4).

3.2. Larval survival and cardiotoxicity

Larval survival at the end of exposure 1 (72 hpf) ranged from 88.9% ± 3.7 to 97.9% ± 1.2 across all treatments and control. Exposure 2 survival at 72 hpf ranged from 69.3% ± 3.4 to 82.2% ± 3.3 (Fig. 1). Exposure 2 survival was consistently lower than exposure 1 survival in both the treatment and control groups. However, survival did not significantly differ between the negative control and oil treatments in either exposure 1 or 2.

Exposure 1 HEWAF treatment (ΣPAH_{50} 3.55–15.45 µg L^{-1}) significantly increased pericardial area by an average fold-change of 2.21 ± 0.08 relative to the control (Fig. 2).

3.3. Gene expression (qPCR)

Expression of 3-hydroxy-3-methylglutaryl-coenzyme A reductase (*hmgcr*), farnesyl-diphosphate farnesyltransferase 1 (*fdft1*), and squalene epoxidase (*sqle*) all followed a similar decreasing trend in oil exposed groups relative to the seawater control. However, mRNA expression in targeted genes related to cholesterol synthesis was not significantly

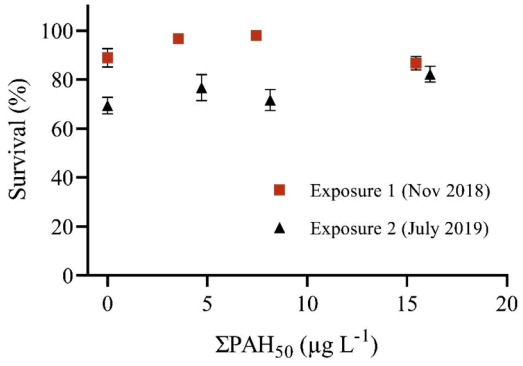

Fig. 1. 72 hpf larval red drum survival following HEWAF exposure. Survival (%) calculated within each exposure beaker. $N = 5$ for exposure 1 control treatment, $n = 6$ for all other treatments. Significant differences were evaluated by Kruskal-Wallis Rank Sum Test. Error bars represent ± SEM.

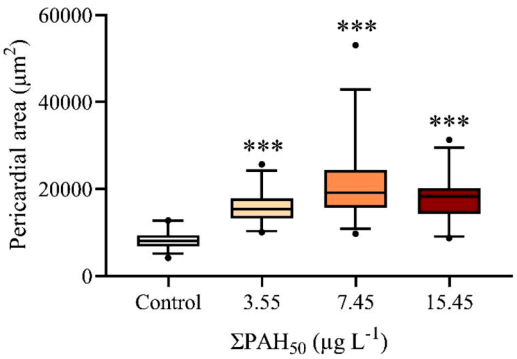

Fig. 2. Pericardial area (μm^2) of 72 hpf red drum larvae from exposure 1 (n = 30 per treatment). Whiskers represent the 5th and 95th percentiles. Data were analysed by a Kruskal-Wallis Rank Sum Test, followed by Dunn's Kruskal-Wallis Test of Multiple Comparisons. ***$p < 0.001$.

altered following HEWAF exposure relative to the control (Fig. 3).

3.4. Total cholesterol quantification

Normalized total cholesterol (cholesterol esters and free cholesterol) displayed an increasing trend in homogenates exposed to HEWAF ΣPAH_{50} 3.55 (37.1 ± 6.0 μg mg^{-1}), 7.45 (33.3 ± 6.5 μg mg^{-1}), 15.45 (34.9 ± 1.7 μg mg^{-1}), relative to the control (25.8 ± 2.1 μg mg^{-1}). However, no significant difference was found among treatments (p = 0.4) (Fig. 4).

3.5. Filipin staining

Mean fluorescence from filipin staining was found to be significantly increased in all HEWAF exposed groups (ΣPAH_{50} 4.71–16.15 μg L^{-1}) relative to the control (81.4 ± 1.0) ($p \leq 0.007$). However, mean fluorescence did not significantly differ between HEWAF exposures (ΣPAH_{50} 4.71(87.3 ± 0.79), 8.15 (88.6 ± 0.80), 16.15 (87.6 ± 0.86) μg L^{-1}) (Fig. 5B). Representative images are presented in Fig. 5A.

4. Discussion

Over the past several years, a number of studies have evaluated the transcriptomic response of developing fish to crude oil exposure. Many of these studies predicted that cholesterol synthesis pathways are affected by oil exposure in early life stage fish, including in red drum (Xu et al., 2017, 2019). In the present study, red drum larvae exposed to *DWH* slick oil displayed elevated free cholesterol levels relative to controls. However, the mRNA transcript abundance of several genes in the cholesterol synthesis pathway was not altered. The discovery of these changes gives evidence that the predicted pathway enhancement in previous transcriptomics studies translates into the disruption of cholesterol, which may contribute to oil-induced maldevelopment of red drum larvae.

Survival of 72 hpf red drum larvae following OFS HEWAF exposure in this study was not significantly reduced, consistent with the estimated 72 hpf red drum LC_{50} of 19.1 μg L^{-1} (Khursigara et al., 2017). However, pericardial area was significantly increased at all concentrations tested (ΣPAH_{50} 3.55 - 15.45 μg L^{-1}), again consistent with an estimated EC_{50} value of 2.4 μg L^{-1} (Khursigara et al., 2017). Though not measured in this study, pericardial edema incidence likely indicates a concurrent reduction in cardiac output and occurrence of craniofacial deformities as these endpoints were found to be similarly sensitive to OFS HEWAF exposure in red drum (Khursigara et al., 2017). The presence of pericardial edema in larvae exposed to crude oil has been linked to reductions in juvenile or adult swimming performance in at least pink salmon, pacific herring, and mahi-mahi (Incardona et al., 2015; Mager et al., 2014). Therefore, the doses used in this study may be relevant to effects at later life stages.

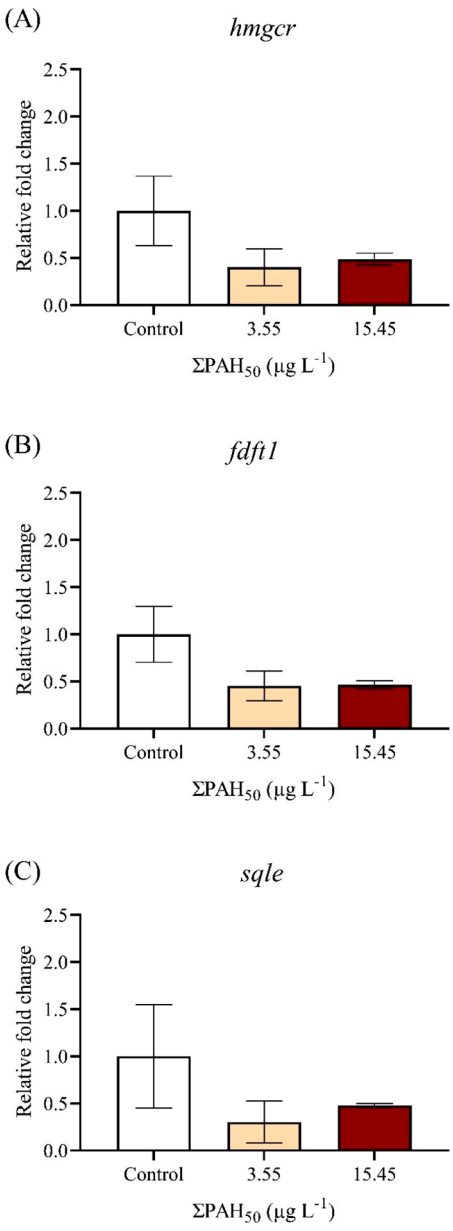

Fig. 3. Relative expression of select genes involved in cholesterol synthesis in 72 hpf larval red drum homogenates from exposure 1 (n = 3 per treatment). Data are shown as relative fold change of (A) *HMG-CoA reductase* (*hmgcr*) (B) *farnesyl-diphosphate farnesyltransferase 1* (*fdft1*), *(C) squalene epoxidase* (*sqle*). Significance was assessed by one-way ANOVA. Error bars represent ± SEM.

Transcriptomic analysis of 72 hpf red drum larvae predicted the cholesterol biosynthesis pathway was enhanced following exposure to ΣPAH_{50} 4.74 μg L^{-1} (Xu et al., 2017). In the present study, we targeted *hmgcr*, *fdft1*, and *sqle* with qPCR. These genes were targeted because they encode enzymes that catalyze critical steps throughout the cholesterol synthesis pathway. *Hmgcr* catalyzes a rate-limiting reaction towards the beginning of the pathway. Enzymes associated with *fdft1* and *sqle* catalyze successive reactions further along in the pathway. Despite previously finding increased expression of *sqle* (log2fold = 1.541; p-value = 2E-07) and *hmgcr* (log2fold = 0.7255; p-value = 8E-06) in 72 hpf HEWAF exposed red drum (Xu et al., 2017), we did not observe significant changes to the expression of these genes in this study (ΣPAH_{50} 3.55–15.45 μg L^{-1}). Here, we targeted *fdft1* because it was

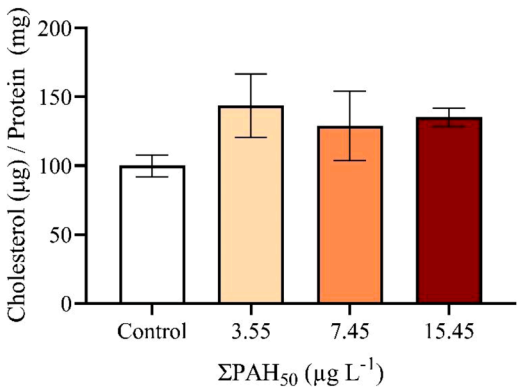

Fig. 4. Total cholesterol (µg) normalized to total protein (mg) in 72 hpf red drum larval homogenates (n = 3 per treatment) from exposure 1. Data were analysed by 1-way ANOVA. Error bars represent ± SEM.

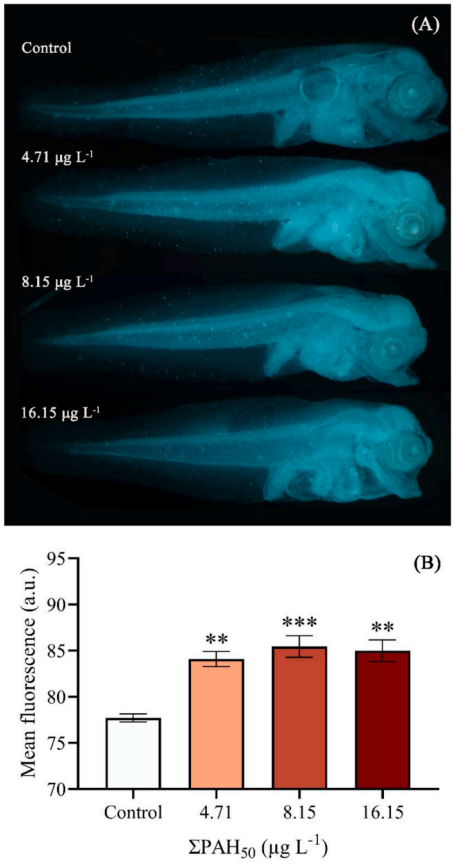

Fig. 5. (A) Representative images of filipin staining for free cholesterol in control and HEWAF exposed 72 hpf red drum larvae from exposure 2. (B) Background corrected mean fluorescence intensity of staining in the larval body (arbitrary units (a.u.)) (n = 3 in control treatment; n = 6 in ΣPAH_{50} 4.71–8.15 µg L^{-1}; n = 5 ΣPAH_{50} 16.15 µg L^{-1}). Statistical significance was determined by 1-way ANOVA. The significance of individual comparisons was determined by Tukey's honestly significant difference test. Error bars represent ± SEM. $^{**}p < 0.01$, $^{***}p < 0.001$.

significantly altered in zebrafish exposed to phenanthrene (McGruer et al., 2021) and diesel WAF (Mu et al., 2018). However, *fdft1* was not altered in red drum exposed to HEWAF (log2fold = 0.159; p-value = 0.499) (Xu et al., 2017), and we did not observe significant changes to *fdft1* expression in this study. Predictions of pathway enhancement in the previous transcriptomic studies were based on enhanced expression throughout the entire cholesterol synthesis pathway, which includes >20 enzymes (Xu et al., 2017). Therefore, there may be molecular changes we are not observing. Moreover, there may be variations between experiments due to differences in dose or variability in embryo yolk composition.

Despite a lack of a measurable difference in transcription, quantifying both total cholesterol and free cholesterol allowed for a better understanding of how oil exposure may affect cholesterol concentration and distribution. Free cholesterol is unesterified cholesterol that can be readily incorporated into cell membranes, while total cholesterol is the sum of both free cholesterol and cholesteryl esters. Interestingly, we found that filipin staining of free cholesterol in whole-mount larvae (whole-body) was significantly increased at all doses tested (ΣPAH_{50} 4.71–16.15 µg L^{-1}). By comparison, total cholesterol measured in larval homogenates was not affected by HEWAF exposure (ΣPAH_{50} 3.55–15.45 µg L^{-1}) but did follow an increasing trend, supporting our findings from filipin staining. Together, these results support predictions that cholesterol is impacted by oil exposure and demonstrates that free cholesterol levels are elevated with crude oil exposure.

Increases in free cholesterol in the absence of differential expression of enzymes in the synthesis pathway have been reported in previous studies (Qian et al., 2018). Cholesterol biosynthesis is a complex and energetically expensive process requiring more than 20 enzymes. Nearly all genes encoding cholesterol synthesis enzymes can be targeted by sterol regulatory element-binding protein (SREBP) transcription factors, which allows for coordinated activation of the pathway. However, processes beyond synthesis regulate cellular cholesterol and may explain the increase in free cholesterol we observed (Sharpe and Brown, 2013). Outside of the transcriptional response, disturbance to cholesterol homeostasis may be produced by disrupting cholesterol transport (i.e., import and export) (Maxfield and Wüstner, 2002), disruption to cholesterol metabolism, or post-transcriptional regulation of cholesterol synthesis enzymes (Sharpe and Brown, 2013). Future studies would need to be conducted to elucidate the mechanism of cholesterol accumulation.

Either increases or decreases in cholesterol can cause adverse effects in both fish and mammals (Campos et al., 2016; Maerz et al., 2019; Maxfield and Tabas, 2005). Interestingly, both depletion and excess cholesterol loading have been implicated in disordered neurodevelopment (Ko et al., 2005), suggesting that sustained excess cholesterol in red drum could impair neurodevelopment. Previously, red drum embryos exposed to ΣPAH_{50} 2.72 µg L^{-1} slick oil displayed a reduced optomotor response (OMR) at 12 days post-hatch relative to controls (Magnuson et al., 2018). Complex neural networks drive OMR, and the resulting behavioral response could be affected by impaired neural development (Naumann et al., 2016). Additionally, larval red drum exposed to *DWH* crude oil displayed increased risk-taking behavior and reduced prey-capture ability, which again could be downstream of impaired cognitive function (Rowsey et al., 2019). Together, these studies suggest a link between neurological development and higher-level behavioral changes which may influence ecological survival.

Additionally, both increases and decreases in free cholesterol have been shown to affect cellular ion movement in cardiomyocytes and other muscle cells by direct or indirect interaction with ion channels (Levitan et al., 2010, 2014). The currently proposed mechanism of cardiac dysfunction in oil-exposed fish is through impairment of Ca^{2+} and K^{+}movement (Brette et al., 2014, 2017), resulting in reduced myocyte contractility (Heuer et al., 2019). Therefore, a buildup of free cholesterol due to oil exposure could disrupt ion channel function and contribute to cardiotoxicity. Ultimately, disruption of heart function can permanently alter morphology and subsequent function (Incardona and Scholz, 2017).

In conclusion, previous studies have shown species- and stage-dependent impacts of oil on cholesterol and/or sterols but could not differentiate between nutrients contained in the unused yolk-sac and

those utilized by the developing larvae (Laurel et al., 2019; McGruer et al., 2019). The present study found that free cholesterol levels are elevated in red drum larvae at a stage where the yolk-sac has been largely absorbed, indicating potential developmental consequences. However, the mechanisms by which cholesterol is elevated are unknown, and the downstream effects of elevated cholesterol should be considered further.

Data availability statement

All data can be freely accessed through the Gulf of Mexico Research Initiative Information & Data Cooperative (GRIIDC) at https://data.gulfresearchinitiative.org (DOI: 10.7266/BCA0N51T).

CRediT authorship contribution statement

Victoria McGruer: Conceptualization, Visualization, Formal analysis, Methodology, Visualization, Data curation, Writing – original draft. **Alexis J. Khursigara:** Formal analysis, Methodology, Visualization, Data curation. **Jason T. Magnuson:** Formal analysis, Methodology, Visualization, Data curation. **Andrew J. Esbaugh:** Formal analysis, Methodology. **Justin B. Greer:** Formal analysis, Methodology, Data curation. **Daniel Schlenk:** Conceptualization, Visualization, Formal analysis, Methodology.

Declaration of Competing Interest

The authors declare that they have no known competing financial interests or personal relationships that could have appeared to influence the work reported in this paper.

Acknowledgment

This work was made possible through a grant from The Gulf of Mexico Research Initiative to the RECOVER II research consortium (Relationship of Effects of Cardiac Outcomes in Fish for Validation of Ecological Risk II); Grant No. SA-1520. The authors would like to thank Kerri Lynn Ackerly for her assistance in image collections for morphological assessment. Any use of trade, firm, or product names is for descriptive purposes only and does not imply endorsement by the U.S. Government.

Supplementary materials

Supplementary material associated with this article can be found, in the online version, at doi:10.1016/j.aquatox.2021.105988.

References

Brette, F., Machado, B., Cros, C., Incardona, J.P., Scholz, N.L., Block, B.a., 2014. Crude oil impairs cardiac excitation-contraction coupling in fish. Science 1681, 772–776. https://doi.org/10.1126/science.1242747 (February).

Brette, F., Shiels, H.A., Galli, G.L.J., Cros, C., Incardona, J.P., Scholz, N.L., Block, B.A., 2017. A novel cardiotoxic mechanism for a pervasive global pollutant. Sci. Rep. 7, 1–9. https://doi.org/10.1038/srep41476.

Campos, L.M., Rios, E.A., Guapyassu, L., Midlej, V., Atella, G.C., Herculano-Houzel, S., Benchimol, M., Mermelstein, C., Costa, M.L., 2016. Alterations in zebrafish development induced by simvastatin: comprehensive morphological and physiological study, focusing on muscle. Exp. Biol. Med. 241 (17), 1950–1960. https://doi.org/10.1177/1535370216659944.

Gimpl, G., & Gehrig-Burger, K. (2007). Cholesterol reporter molecules. In Biosci. Rep. (Vol. 27, Issue 6, pp. 335–358). 10.1007/s10540-007-9060-1.

Hölttä-Vuori, M., Uronen, R.L., Repakova, J., Salonen, E., Vattulainen, I., Panula, P., Li, Z., Bittman, R., Ikonen, E., 2008. BODIPY-cholesterol: a new tool to visualize sterol trafficking in living cells and organisms. Traffic 9 (11), 1839–1849. https://doi.org/10.1111/j.1600-0854.2008.00801.x.

Heuer, R.M., Galli, G.L.J., Shiels, H.A., Fieber, L.A., Cox, G.K., Mager, E.M., Stieglitz, J. D., Benetti, D.D., Grosell, M., Crossley, D.A., 2019. Impacts of *Deepwater Horizon* crude oil on mahi-mahi (Coryphaena hippurus) heart cell function. Environ. Sci. Technol. 53 (16), 9895–9904. https://doi.org/10.1021/acs.est.9b03798.

Hicken, C.E., Linbo, T.L., Baldwin, D.H., Willis, M.L., Myers, M.S., Holland, L., Larsen, M., Stekoll, M.S., Rice, S.D., Collier, T.K., Scholz, N.L., Incardona, J.P., 2011. Sublethal exposure to crude oil during embryonic development alters cardiac morphology and reduces aerobic capacity in adult fish. Proc. Natl. Acad. Sci. 108 (17), 7086–7090. https://doi.org/10.1073/pnas.1019031108.

Hu, Y.H., Zheng, W.J., Sun, L, 2010. Identification and molecular analysis of a ferritin subunit from red drum (*Sciaenops ocellatus*). Fish Shellfish Immunol. 28 (4), 678–686. https://doi.org/10.1016/J.FSI.2010.01.001.

Incardona, J.P., Scholz, N.L., 2017. Environmental pollution and the fish heart. Fish Physiol. 36 (PartB), 373–433. https://doi.org/10.1016/bs.fp.2017.09.006.

Incardona, J.P., Scholz, N.L., Burggren, W., Dubansky, B., 2018. Case study: the 2010 *Deepwater Horizon* oil spill and its environmental developmental impacts. Eds. Development and Environment. Springer International Publishing, pp. 235–283. https://doi.org/10.1007/978-3-319-75935-7.

Incardona, J.P., Swarts, T.L., Edmunds, R.C., Linbo, T.L., Aquilina-Beck, A., Sloan, C.A., Gardner, L.D., Block, B.A., Scholz, N.L., 2013. Exxon valdez to *Deepwater Horizon*: comparable toxicity of both crude oils to fish early life stages. Aquat. Toxicol. 142–143, 303–316. https://doi.org/10.1016/j.aquatox.2013.08.011.

Incardona, J.P., Carls, M.G., Holland, L., Linbo, T.L., Baldwin, D.H., Myers, M.S., Peck, K. A., Tagal, M., Rice, S.D., Scholz, N.L., 2015. Very low embryonic crude oil exposures cause lasting cardiac defects in salmon and herring. Sci. Rep. 5 https://doi.org/10.1038/srep13499.

Jones, E.R., Simning, D., Serafin, J., Sepúlveda, M.S., Griffitt, R.J., 2020. Acute exposure to oil induces age and species-specific transcriptional responses in embryo-larval estuarine fish. Environ. Pollut. 263. https://doi.org/10.1016/j.envpol.2020.114325 (April).

Khursigara, A.J., Perrichon, P., Martinez Bautista, N., Burggren, W.W., Esbaugh, A.J., 2017. Cardiac function and survival are affected by crude oil in larval red drum, *Sciaenops ocellatus*. Sci. Total Environ. 579, 797–804. https://doi.org/10.1016/j.scitotenv.2016.11.026 (April 2017).

Ko, M., Zou, K., Minagawa, H., Yu, W., Gong, J.S., Yanagisawa, K., Michikawa, M., 2005. Cholesterol-mediated neurite outgrowth is differently regulated between cortical and hippocampal neurons. J. Biol. Chem. 280 (52), 42759–42765. https://doi.org/10.1074/jbc.M509164200.

Laurel, B.J., Copeman, L.A., Iseri, P., Spencer, M.L., Hutchinson, G., Nordtug, T., Donald, C.E., Meier, S., Allan, S.E., Boyd, D.T., Ylitalo, G.M., Cameron, J.R., French, B.L., Linbo, T.L., Scholz, N.L., Incardona, J.P., 2019. Embryonic crude oil exposure impairs growth and lipid allocation in a keystone arctic forage fish. IScience 19, 1101–1113. https://doi.org/10.1016/j.isci.2019.08.051 (August).

Levitan, I., Singh, D.K., Rosenhouse-Dantsker, A., 2014. Cholesterol binding to ion channels. In: Front. Physiol., 5 https://doi.org/10.3389/fphys.2014.00065. FEBFrontiers Media SA.

Levitan, I., Fang, Y., Resenhouse-Dantsker, A., Romanenko, V., 2010. Choleterol and ion channels. In J. Chem. Inf. Model. 51 (9). https://doi.org/10.1007/978-90-481-8622-8.

Livak, K.J., Schmittgen, T.D., 2001. Analysis of relative gene expression data using real-time quantitative PCR and the 2-ΔΔCT method. Methods 25 (4), 402–408. https://doi.org/10.1006/meth.2001.1262.

Maerz, L.D., Burkhalter, M.D., Schilpp, C., Wittekindt, O.H., Frick, M., Philipp, M., 2019. Pharmacological cholesterol depletion disturbs ciliogenesis and ciliary function in developing zebrafish. Commun. Biol. 2 (1), 1–13. https://doi.org/10.1038/s42003-018-0272-7.

Mager, E.M., Esbaugh, A.J., Stieglitz, J.D., Hoenig, R., Bodinier, C., Incardona, J.P., Scholz, N.L., Benetti, D.D., Grosell, M., 2014. Acute embryonic or juvenile exposure to *Deepwater Horizon* crude oil impairs the swimming performance of mahi-mahi (Coryphaena hippurus). Environ. Sci. Technol. 48 (12), 7053–7061. https://doi.org/10.1021/es501628k.

Magnuson, J.T., Khursigara, A.J., Allmon, E.B., Esbaugh, A.J., Roberts, A.P., 2018. Effects of *Deepwater Horizon* crude oil on ocular development in two estuarine fish species, red drum (*Sciaenops ocellatus*) and sheepshead minnow (Cyprinodon variegatus). Ecotoxicol. Environ. Saf. 166, 186–191. https://doi.org/10.1016/j.ecoenv.2018.09.087.

Maxfield, F.R., Tabas, I., 2005. Role of cholesterol and lipid organization in disease. In Nature 438 (7068), 612–621. https://doi.org/10.1038/nature04399.

Maxfield, F.R., Wüstner, D., 2002. Intracellular cholesterol transport. J Clin Invest 110 (7), 891–898. https://doi.org/10.1172/JCI200216500.

McGruer, V., Pasparakis, C., Grosell, M., Stieglitz, J.D., Benetti, D.D., Greer, J.B., Schlenk, D., 2019. *Deepwater Horizon* crude oil exposure alters cholesterol biosynthesis with implications for developmental cardiotoxicity in larval mahi-mahi (Coryphaena hippurus). Comp. Biochem. Physiol. Part C Toxicol. Pharmacol. 220, 31–35. https://doi.org/10.1016/j.cbpc.2019.03.001 (March).

McGruer, V., Tanabe, P., Vliet, S.M.F., Dasgupta, S., Qian, L., Volz, D.C., Schlenk, D., 2021. Effects of phenanthrene exposure on cholesterol homeostasis and cardiotoxicity in zebrafish embryos. Environ. Toxicol. Chem. 00 (00), 1–10. https://doi.org/10.1002/etc.5002.

Michel, J., Owens, E.H., Zengel, S., Graham, A., Nixon, Z., Allard, T., Holton, W., Reimer, P.D., Lamarche, A., White, M., Rutherford, N., Childs, C., Mauseth, G., Challenger, G., Taylor, E., 2013. Extent and degree of shoreline oiling: *Deepwater Horizon* oil spill, gulf of Mexico, USA. PLoS ONE 8 (6), e65087. https://doi.org/10.1371/journal.pone.0065087.

Mu, X., Liu, J., Yang, K., Huang, Y., Li, X., Yang, W., Qi, S., Tu, W., Shen, G., Li, Y., 2018. Diesel water-accommodated fraction induced lipid homeostasis alteration in zebrafish embryos. Environ. Pollut. 242, 952–961. https://doi.org/10.1016/j.envpol.2018.07.055.

National Marine Fisheries, Service., 2018. Fisheries Economics of the United States, 2016, NMFS-F/SPO-187,. U.S. Dept. of Commerce, NOAA Tech. Memo, pp. 243–p. https://www.fisheries.noaa.gov/content/fisheries-economics-united-states-2016.

Naumann, E.A., Fitzgerald, J.E., Dunn, T.W., Rihel, J., Sompolinsky, H., Engert, F., 2016. From whole-brain data to functional circuit models: the zebrafish optomotor response. Cell 167 (4), 947–960. https://doi.org/10.1016/j.cell.2016.10.019 e20.

Nixon, Z., Zengel, S., Baker, M., Steinhoff, M., Fricano, G., Rouhani, S., Michel, J., 2016. Shoreline oiling from the *Deepwater Horizon* oil spill. Mar. Pollut. Bull. 107 (1), 170–178. https://doi.org/10.1016/j.marpolbul.2016.04.003.

Qian, L., Cui, F., Yang, Y., Liu, Y., Qi, S., Wang, C., 2018. Mechanisms of developmental toxicity in zebrafish embryos (Danio rerio) induced by boscalid. Sci. Total Environ. 634, 478–487. https://doi.org/10.1016/j.scitotenv.2018.04.012.

R Core Team (2020). R: A language and environment for statistical computing. R Foundation for Statistical Computing, Vienna, Austria. URL https://www.R-project.org/.

Rooker, J.R., Kitchens, L.L., Dance, M.A., Wells, R.J.D., Falterman, B., Cornic, M., 2013. Spatial, temporal, and habitat-related variation in abundance of pelagic fishes in the gulf of Mexico: potential Implications of the *Deepwater Horizon* Oil Spill. PLoS ONE 8 (10), e76080. https://doi.org/10.1371/journal.pone.0076080.

Rowsey, L.E., Johansen, J.L., Khursigara, A.J., Esbaugh, A.J., 2019. Oil exposure impairs predator-prey dynamics in larval red drum (*Sciaenops ocellatus*). Mar. Freshw. Res. 71 (1), 99–106. https://doi.org/10.1071/MF18263.

Sørensen, L., Sørhus, E., Nordtug, T., Incardona, J.P., Linbo, T.L., Giovanetti, L., Karlsen, Ø., Meier, S., 2017. Oil droplet fouling and differential toxicokinetics of polycyclic aromatic hydrocarbons in embryos of Atlantic haddock and cod. PLoS ONE 12 (7), 1–26. https://doi.org/10.1371/journal.pone.0180048.

Sharpe, L.J., Brown, A.J., 2013. Controlling cholesterol synthesis beyond 3-hydroxy-3-methylglutaryl-CoA reductase (HMGCR). J. Biol. Chem. 288 (26), 18707–18715. https://doi.org/10.1074/jbc.R113.479808.

Sun, B.guang, Chi, H., 2016. Cathepsin S of *Sciaenops ocellatus*: identification, transcriptional expression and enzymatic activity. Int. J. Biol. Macromol. 82, 76–82. https://doi.org/10.1016/J.IJBIOMAC.2015.10.037.

Tabas, I., 2002. Consequences of cellular cholesterol accumulation: basic concepts and physiological implications. J. Clin. Investig. 110 (7), 905–911. https://doi.org/10.1172/JCI0216452.

Deepwater Horizon Natural Resource Damage Assessment Trustees, 2016. Deepwater Horizon Oil Spill: Final Programmatic Damage Assessment and Restoration Plan (PDARP) and Final Programmatic Environmental Impact Statement (PEIS). http://www.gulfspillrestoration.noaa.gov/restorationplanning/gulf-plan/.

Xu, Elvis G., Mager, E.M., Grosell, M., Pasparakis, C., Schlenker, L.S., Stieglitz, J.D., Benetti, D., Hazard, E.S., Courtney, S.M., Diamante, G., Freitas, J., Hardiman, G., Schlenk, D., 2016. Time- and oil-dependent transcriptomic and physiological responses to *Deepwater Horizon* oil in mahi-mahi (Coryphaena hippurus) embryos and larvae. Environ. Sci. Technol. 50 (14), 7842–7851. https://doi.org/10.1021/acs.est.6b02205.

Xu, Elvis Genbo;, Khursigara, A.J.., Magnuson, J., Hazard, E.S.S., Hardiman, G., Esbaugh, A.J.., Roberts, A.P., Schlenk, D, 2017. Larval red drum (*Sciaenops ocellatus*) sublethal exposed to weathered *Deepwater Horizon* crude oil: developmental and trscriptomic consequences. Environ. Sci. Technol. 51 (17), 10162–10172. https://doi.org/10.1021/acs.est.7b02037.

Xu, Elvis Genbo, Khursigara, A.J., Li, S., Esbaugh, A.J., Dasgupta, S., Volz, D.C., Schlenk, D, 2019. MRNA-miRNA-Seq reveals neuro-cardio mechanisms of crude oil toxicity in red drum (*Sciaenops ocellatus*). Environ. Sci. Technol. 53 (6), 3296–3305. https://doi.org/10.1021/acs.est.9b00150.